

1-31-2020

Highly active cationic cobalt(II) hydroformylation catalysts

Drew M. Hood
Louisiana State University

Ryan A. Johnson
Louisiana State University

Alex E. Carpenter
Exxon Mobil Corporation

Jarod M. Younker
Exxon Mobil Corporation

David J. Vinyard
Louisiana State University

See next page for additional authors

Follow this and additional works at: https://digitalcommons.lsu.edu/biosci_pubs

Recommended Citation

Hood, D., Johnson, R., Carpenter, A., Younker, J., Vinyard, D., & Stanley, G. (2020). Highly active cationic cobalt(II) hydroformylation catalysts. *Science*, 367 (6477), 542-548. <https://doi.org/10.1126/science.aaw7742>

This Article is brought to you for free and open access by the Department of Biological Sciences at LSU Digital Commons. It has been accepted for inclusion in Faculty Publications by an authorized administrator of LSU Digital Commons. For more information, please contact ir@lsu.edu.

Authors

Drew M. Hood, Ryan A. Johnson, Alex E. Carpenter, Jarod M. Younker, David J. Vinyard, and George G. Stanley

CATALYSIS

Highly active cationic cobalt(II) hydroformylation catalysts

Drew M. Hood¹, Ryan A. Johnson¹, Alex E. Carpenter², Jarod M. Younker², David J. Vinyard³, George G. Stanley^{1*}

The cobalt complexes $\text{HCo}(\text{CO})_4$ and $\text{HCo}(\text{CO})_3(\text{PR}_3)$ were the original industrial catalysts used for the hydroformylation of alkenes through reaction with hydrogen and carbon monoxide to produce aldehydes. More recent and expensive rhodium-phosphine catalysts are hundreds of times more active and operate under considerably lower pressures. Cationic cobalt(II) bisphosphine hydrido-carbonyl catalysts that are far more active than traditional neutral cobalt(I) catalysts and approach rhodium catalysts in activity are reported here. These catalysts have low linear-to-branched (L:B) regioselectivity for simple linear alkenes. However, owing to their high alkene isomerization activity and increased steric effects due to the bisphosphine ligand, they have high L:B selectivities for internal alkenes with alkyl branches. These catalysts exhibit long lifetimes and substantial resistance to degradation reactions.

Hydroformylation, or the oxo reaction, is one of the highest-volume homogeneously catalyzed industrial processes today, converting alkenes, H_2 , and CO into aldehydes (and related products) at a rate of more than 10 million metric tons per year (1). The four most common industrial catalyst technologies are summarized in Table 1 (1–3), along with the cationic Co(II) bisphosphine system reported here. Although these major industrial catalyst systems exhibit distinctive strengths and perform optimally under specific conditions, a long-standing challenge has been to access the feed tolerance and robustness of so-called high-pressure systems [i.e., $\text{HCo}(\text{CO})_4$] under mild conditions with base metals.

The first hydroformylation catalyst, cobalt complex $\text{HCo}(\text{CO})_4$, was accidentally discovered by Otto Roelen in 1938; its currently accepted mechanism was proposed by Heck and Breslow in 1960 (4, 5). The $\text{HCo}(\text{CO})_4$ -catalyzed process is commonly referred to as the high-pressure system because CO partial pressure must be increased drastically as the temperature rises in order to inhibit decomposition of the catalyst to cobalt metal (6).

The phosphine-modified cobalt catalyst system, $\text{HCo}(\text{CO})_3(\text{PR}_3)$, was discovered and commercialized by Slaugh and Mullineaux in the 1960s (7, 8). The electron-donating alkylated phosphine improves catalyst stability by increasing π -backbonding to the carbonyl ligands, which stabilizes the catalyst relative to $\text{HCo}(\text{CO})_4$, allowing it to be run at lower pressures. The stronger Co–CO bonding, however, substantially slows the catalyst, necessitating higher operating temperatures and unusually high

catalyst concentrations (Table 1). The donating phosphine ligand increases the hydrogenation activity of the catalyst for aldehyde-to-alcohol (desired) and alkene-to-alkane (undesired) conversion.

In the early 1970s, rhodium catalysts were discovered to be hundreds of times more active than cobalt for the hydroformylation of linear 1-alkenes (9, 10). However, these systems perform comparatively poorly with branched or otherwise complex olefin streams. Although $\text{HRh}(\text{CO})_4$ is the most active hydroformylation catalyst known, as well as an active alkene isomerization catalyst, it readily forms inactive Rh-carbonyl clusters (1, 11) and requires very high operating pressures. The industry standard for low-pressure hydroformylation is $\text{HRh}(\text{CO})(\text{PPh}_3)_2$ (1, 12). However, facile dissociation of the PPh_3 ligand requires excess PPh_3 (e.g., 0.4 to 1.6 M PPh_3 with 1 mM Rh catalyst) to maintain the most regioselective, albeit lower-activity, bisphosphine catalyst. The high cost and low abundance of rhodium requires low-loss catalyst recycling technologies (1, 6, 12).

Our laboratory previously reported a highly active and selective dicationic dirhodium hydroformylation catalyst bearing a tetraphosphine ligand, $(\text{Et}_2\text{PCH}_2\text{CH}_2)(\text{Ph})\text{PCH}_2\text{P}(\text{Ph})\text{CH}_2\text{CH}_2\text{PEt}_2$, that bridges and chelates the two rhodium centers (13, 14). The chiral diastereomer (used as a racemic mixture) of this catalyst showed high activity and selectivity for the hydroformylation of 1-hexene, while the meso diastereomer was a very poor catalyst. The activity of the chiral diastereomer is a function of bimetallic cooperativity, which is blocked for the meso diastereomer. The localized cationic charges on the metal centers play an important role to compensate for the electron-donating alkylated phosphine ligands that produce poor monometallic rhodium hydroformylation catalysts. Unfortunately, the dicationic dirhodium catalyst suffers from degradation pathways that

lead to catalyst deactivation. A tetraphosphine ligand with a far stronger chelate effect was synthesized, and studies with model nickel complexes using both ligand diastereomers demonstrated the enhanced stability toward phosphine ligand dissociation (15).

The strong chelate effect of this newly synthesized tetraphosphine ligand prompted us to prepare and study a dicationic dicobalt(II) catalyst precursor, $[\text{Co}_2(\text{acac})_2(\text{P4-phenylene})](\text{BF}_4)_2$ [acac, acetoacetate; P4-phenylene, $(\text{Et}_2\text{P})(1,2\text{-C}_6\text{H}_4)\text{P}(\text{Ph})\text{CH}_2\text{P}(\text{Ph})(1,2\text{-C}_6\text{H}_4)(\text{PEt}_2)$], for hydroformylation activity (Fig. 1). This system proved to be quite active for hydroformylation, but both the chiral and meso diastereomers exhibited similar activity and selectivity (supplementary materials, table S1). This observation indicated that the dicobalt catalyst was functioning as two independent monometallic catalysts, because from the dirhodium catalysis only the chiral diastereomer can effectively promote bimetallic cooperativity. This prompted the study of much simpler monometallic cationic Co(II) bisphosphine precursors.

A class of cationic monometallic cobalt catalysts

The monometallic catalyst precursor, $[\text{Co}(\text{acac})(\text{DPPBz})](\text{BF}_4)$ (Fig. 1), proved to be even more active than the dicobalt complexes for hydroformylation under exceptionally mild conditions for cobalt. Table 2 shows the role of temperature and pressure for the hydroformylation of 1-hexene using $[\text{Co}(\text{acac})(\text{DPPBz})](\text{BF}_4)$ as the catalyst precursor (average of three catalytic runs). Activity increased with temperature up to 170°C at 50 bar of 1:1 H_2 :CO, at which point catalyst decomposition commenced. This cationic Co(II) catalyst showed high alkene isomerization activity, similar to Co(I) systems. The low linear-to-branched (L:B) selectivity observed for the aldehyde products demonstrates that the cationic cobalt catalyst can coordinate internal alkenes formed through isomerization and hydroformylate them (full analysis of the branched aldehyde and alkene products is given in table S2). The highest alkene isomerization activity occurred at relatively high temperatures and low pressures (160°C and 30 bar), which is consistent with most hydroformylation catalysts (1, 6, 12). Hydrogenation of aldehyde product to alcohol was occasionally observed despite using a 1:1 H_2 :CO gas ratio that does not favor hydrogenation. Alcohol production was more prevalent with the more electron-donating bisphosphine ligands at higher temperatures (e.g., 160°C) in the 30- to 60-bar pressure regime once the aldehyde concentration built up (tables S1 and S6). Hydrogenation of alkene to alkane was usually <3%.

The observed CO pressure effect (Table 2) appears notable. As the H_2 :CO pressure increased, the catalyst activity also increased. The initial turnover frequency (TOF) for the

¹Department of Chemistry, Louisiana State University, Baton Rouge, LA 70803, USA. ²ExxonMobil Chemical Company, Baytown, TX 77520, USA. ³Department of Biological Sciences, Louisiana State University, Baton Rouge, LA 70803, USA.

*Corresponding author. Email: gstanley@lsu.edu

cobalt-DPPBz-based catalyst essentially doubled from 52.5 min⁻¹ (30 bar) to 103.2 min⁻¹ (90 bar). Hydroformylation catalysts generally exhibit a negative [CO] order rate dependence (e.g., -0.6 to -1) beyond a critical CO pressure (1, 6, 12) owing to the inhibition noted above.

However, preliminary kinetic data using 3,3-dimethylbutene as an alkene that cannot be isomerized showed that reaction rates are first order in cobalt catalyst and alkene, approximately +0.6 in H₂, and -1 in CO (table S3). The drastic increase in TOF with increasing H₂:CO pressure for 1-hexene shown in Table 2 is due to the lower alkene isomerization reaction at higher pressures, which increases the amount of the most-active 1-alkene present relative to the considerably less reactive internal alkenes formed from alkene isomerization.

Electron-rich bisphosphine ligands lead to more active cationic Co(II) hydroformylation catalysts at lower to medium H₂:CO pressures (table S4). The most electron-rich Et₂PCH₂CH₂PEt₂ (depe) ligand generates a catalyst that is 46% more active compared with the DPPBz system at 51.7 bar and 140°C (table S4). This is very unusual, as electron-donating phosphines, especially chelating bisphosphines, are well known to substantially lower the activity of both rhodium and cobalt monometallic hydroformylation catalysts. The more electron-donating phosphine-based Co(II) catalysts do show a stronger CO inhibitor effect at higher pressures. The (Et₂P)₂-1,2-C₆H₄ (DEPBz) ligand-based cationic cobalt catalyst, for example, has an initial TOF of 61.5 min⁻¹ at 50 bar and 140°C, but that rate

slows to 36.7 min⁻¹ at 70 bar and 21.7 min⁻¹ at 90 bar (table S5).

High activity at low pressure

The higher activity of the more electron-rich cationic Co(II) bisphosphine catalysts allows operation at the low pressures typical of rhodium catalysis. Using [Co(acac)(depe)](BF₄) under our standard conditions (1 mM catalyst, 1 M 1-hexene, dimethoxytetraglyme solvent), the catalyst was activated at 140°C under 34 bar of 1:1 H₂:CO for 5 min. The autoclave temperature and pressure were then reduced to 100°C and 10 bar, followed by pressure injection of 1-hexene to initiate catalysis. Sixty-eight turnovers (TOs) to aldehyde [gas chromatography-mass spectrometry (GC-MS) analysis] were observed after 1 hour and 619 TOs after 29 hours, with a

Table 1. Comparison of industrial hydroformylation catalysts and the cationic Co(II) bisphosphine system. TOF, turnover frequency; L:B, product linear-to-branched ratio.

Properties	Unmodified Co(I)	Phosphine-modified Co(I)	Unmodified Rh(I)	Phosphine-modified Rh(I)	Cationic Co(II) bisphosphine
Catalyst	HCo(CO) ₄	HCo(CO) ₃ (PR ₃)	HRh(CO) ₄	HRh(CO)(PPh ₃) ₂	[HCo(CO) _n (P ₂)] ⁺
Typical alkene feed	Branched and/or internal olefins	Linear alkenes (α or internal)	Branched and/or internal olefins	Shorter-chain α-olefins and specialty substrates	Branched and/or internal olefins
Temperature (°C)	140–200	180–200	100–150	80–130	100–160
Pressure (bar)	100–300	50–150	100–300	8–20	10–50
Ligand:metal ratio	—	2:1	—	400–1600:1	1:1
Ligand type	—	Alkyl phosphine	—	PPh ₃ (most common)	Diphosphine
Catalyst loading (ppm metal)	500–1500	1000–2500	1–10	10–250	60–600
H ₂ :CO ratio	1:1	2:1	1:1	1.2:1	1:1
Typical TOF (min ⁻¹) for α-olefins	5–20	0.2–0.5	>150	40–600	10–60
L:B (n:iso)	1–4:1	8–10:1	1–2:1	10–20:1	1–2:1
Alkene isomerization	High	Moderate	Low to moderate	Low	High
By-product formation	High (up to 30% alcohols, paraffin, acetals, etc.)	20–30% paraffin	Low	Very low	Low

Table 2. Temperature- and pressure-dependent studies for the hydroformylation of 1-hexene with [Co(acac)(DPPBz)](BF₄). DPPBz, (Ph₂P)₂-1,2-C₆H₄. Catalysis conditions: 1 mM catalyst (61 ppm Co), 1 M 1-hexene, 0.1 M heptane standard, dimethoxytetraglyme solvent, 1:1 H₂:CO, 1000 revolutions per minute stirring under constant pressure. TOF based on a sample taken at 2 min. Other results based on sampling after 1 hour.

Temperature (°C)	Pressure (bar)	Initial TOF (min ⁻¹)	Aldehyde (%)	Aldehyde L:B	Alkane (%)	Isomerization (%)
120*	50	26.5	59.4	1.7	0	7.6
140*	50	43.6	71.3	1.3	0.3	17.9
160	50	66.0	76.8	1.1	1.4	18.9
Pressure (bar)	Temperature (°C)	Initial TOF (min ⁻¹)	Aldehyde (%)	Aldehyde L:B	Alkane (%)	Isomerization (%)
30†	160	52.5	49.0	0.94	1.4	45.7
50	160	66.0	76.8	1.1	1.4	18.9
70	160	94.8	84.0	1.3	1.2	12.1
90	160	103.2	87.3	1.4	1.0	9.1

*The reaction mixture was heated to 160°C for 5 min to activate the catalyst, then cooled to operating temperature before alkene injection.

†Some catalyst decomposition was noted by black cobalt metal deposition.

L:B aldehyde ratio of 0.8, no detectable alkane or alcohol production, and 15.1% alkene isomerization. The cationic Co(II) bisphosphine catalyst is far faster than the recently reported $\text{H}_2\text{Fe}(\text{CO})_2(\text{PPh}_3)_2$ catalyst, which underwent only 95 TOs with 1-octene over 24 hours at 100°C and 20 bar with 2:1 L:B aldehyde regioselectivity (16).

Direct rate comparisons between the cationic cobalt(II) bisphosphine catalysts reported here and industrial cobalt systems are difficult because of the higher pressure or temperature conditions used in industry and differences in catalyst stability. The high-pressure $\text{HCo}(\text{CO})_4$ catalyst, for example, decomposes to cobalt metal under the medium-pressure conditions reported in Table 1 (table S6). The phosphine-modified $\text{HCo}(\text{PR}_3)(\text{CO})_3$ catalyst is run industrially at higher temperatures and rather high catalyst and phosphine ligand concentrations relative to our 1 mM [61 parts per million (ppm) Co] catalyst conditions. After 10 minutes, catalytic runs using 1-hexene with a model Co(I) catalyst using PBu_3 under industrial conditions [2400 ppm Co, 75% 1-hexene, 25% tetrahydrofuran (THF), 200°C, 69 bar, 2:1 H_2 :CO] produced 13 TOs to aldehyde (6.4:1 L:B), 41 TOs to alcohol, 35.9% alkene isomerization, and 3.7%

hydrogenation of alkene to alkane. Therefore, the cationic cobalt DPPBz catalyst is at least 30 to 60 times faster than typical phosphine-modified neutral Co(I) catalyst systems.

Table 3 shows hydroformylation results using 3,3-dimethylbutene as the alkene substrate with four different cationic cobalt(II) bisphosphine catalysts and two rhodium-based catalysts using triphenylphosphine (PPh_3) and the bulky, chelating bisphosphite ligand biphenphos (Fig. 1). The Rh-biphenphos-type catalyst is one of the most active and selective hydroformylation catalysts but suffers from facile phosphite degradation reactions that lead to shorter catalyst lifetimes (1, 17–19). We chose 3,3-dimethylbutene as the substrate for these studies to allow a direct comparison of the intrinsic hydroformylation reaction rates between the cationic cobalt bisphosphine and rhodium-based catalysts. The cobalt catalysts are very active at alkene isomerization, which competes with hydroformylation and produces internal alkenes that hydroformylate more slowly. Because of its tertiary carbon center, 3,3-dimethylbutene is not susceptible to alkene isomerization, thus allowing a direct comparison for the hydroformylation activity of these catalysts.

The data in Table 3 demonstrate that the more active cationic cobalt catalysts based on the stronger σ -donating ethyl-substituted bisphosphine ligands (depe and DEPbz) (Fig. 1) are within a factor of 10 of the rhodium catalysts on the basis of the observed rate constant k_{obs} . The reactions with cobalt catalysts were run at a higher temperature and pressure, with the higher temperature probably having more influence on the rate. Therefore, the cobalt catalyst rates are within a factor of ~20 of these rhodium catalysts, although rhodium is >4000 times more expensive than cobalt on a molar basis (20). The increased activity of the cationic Co(II) bisphosphine catalyst system with more electron-donating alkylated phosphines, once again, is very unusual, as both Co(I) and especially Rh(I) hydroformylation catalysts are drastically slowed by electron-donating phosphine ligands owing to stronger metal-carbonyl π -backbonding.

The utility of this cationic cobalt(II) catalyst system is most evident with respect to internal, branched alkenes that are more challenging to hydroformylate (21). The hydroformylation of internal and internal branched alkenes makes up ~20% of the commercial marketplace, using mainly the high-pressure $\text{HCo}(\text{CO})_4$ and $\text{HRh}(\text{CO})_4$ catalyst systems. Table 4 shows the results after 6 hours for three internal branched alkenes using $\text{HCo}(\text{CO})_4$, $[\text{HCo}(\text{CO})_x(\text{depe})](\text{BF}_4)$, Rh: PPh_3 (1:400), and Rh:biphenphos (1:3) catalysts. As might be expected, $\text{HCo}(\text{CO})_4$ has the highest activity for these sterically hindered alkenes, which is why it is used in industry along with the high-pressure $\text{HRh}(\text{CO})_4$ catalyst system. Note, however, that $\text{HCo}(\text{CO})_4$ is running at 90 bar and would slowly decompose to cobalt metal at lower pressures. The $[\text{Co}:\text{depe}]^+$ cationic catalyst is almost as active as $\text{HCo}(\text{CO})_4$ but is operating at a pressure of only 30 bar and would run substantially faster at higher pressures and temperatures (Table 1). The cationic Co(II) catalyst system, like the $\text{HCo}(\text{CO})_4$ system, is selective toward the more valuable linear aldehyde products.

Phosphine-modified rhodium hydroformylation catalysts perform poorly with internal branched alkenes, as seen in Table 4. Neither Rh: PPh_3 nor the highly active rhodium-bisphosphite catalyst systems can hydroformylate 2,3-dimethyl-2-butene (tetramethylethylene), and Rh:biphenphos barely works with 4,4-dimethyl-2-pentene, with only 0.8% conversion after 6 hours. Rh:biphenphos can hydroformylate 4-methyl-2-pentene with excellent selectivity (28:1 L:B), but it completely decomposed and stopped hydroformylating 3 hours into the run. Rh: PPh_3 converted more 4-methyl-2-pentene relative to $[\text{Co}:\text{depe}]^+$, 62.0 versus 54.7% conversion to aldehyde, but with low L:B selectivity (0.4:1 versus 4.4:1).

Stability is a key criterion for judging the overall quality of a catalyst system. For example,

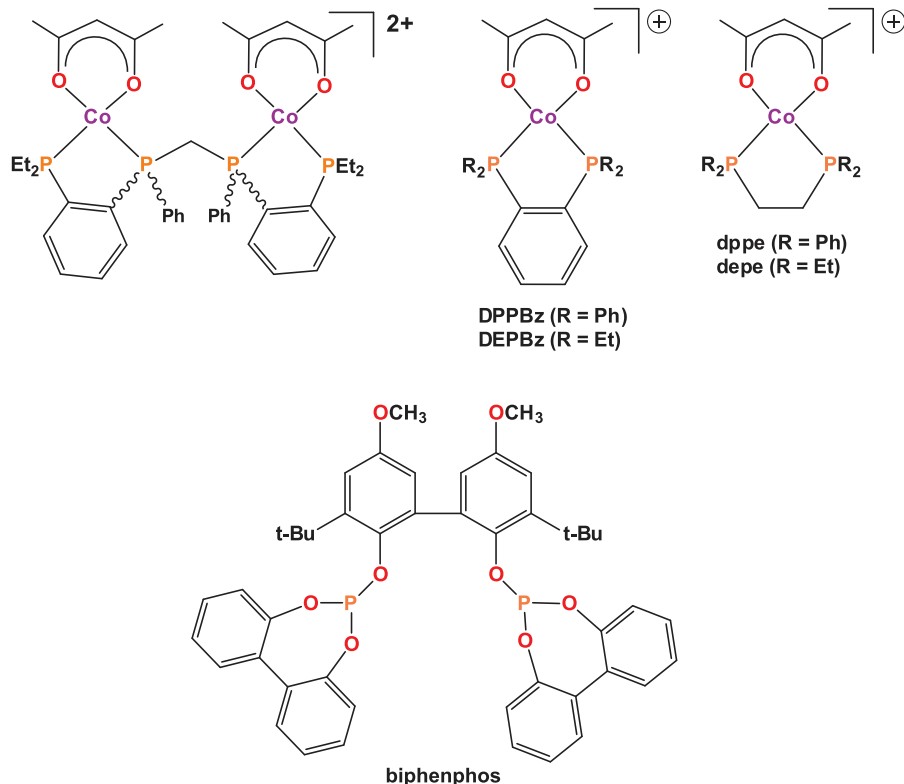


Fig. 1. Structures of the cobalt catalyst precursors and biphenphos ligand in this study. (Top, left to right) $[\text{Co}_2(\text{acac})_2(\text{P4-phenylene})]^{2+}$, $[\text{Co}(\text{acac})(\text{R}_2\text{P-1,2-C}_6\text{H}_4)]^+$, and $[\text{Co}(\text{acac})(\text{R}_2\text{PCH}_2\text{CH}_2\text{PR}_2)]^+$ ($\text{R} = \text{Et}$ or Ph). BF_4^- counteranions are present for each complex. Bisphosphine ligand abbreviations are shown. The biphenphos ligand (bottom) was used for the rhodium catalyst comparison. Et, ethyl; Ph, phenyl; t-Bu, *tert*-butyl.

Rh:PPh₃ catalyst systems operate with a large excess of PPh₃ to minimize Rh-induced phosphine fragmentation reactions that lead to catalyst deactivation (22, 23). Unsaturated rhodium centers are quite active for phosphine P-phenyl, P-benzyl, or P-OR group oxidative addition reactions that initiate several possible catalyst decomposition pathways.

The cationic cobalt bisphosphine catalysts reported here, however, show prolonged stability at moderate temperatures (140° to 160°C) and pressures (50 bar). Unlike for all other known phosphine-modified cobalt and rhodium catalysts, it is not necessary to add excess phosphine ligand to stabilize this cationic cobalt(II) catalyst system. The bisphosphines based on the 1,2-phenylene chelate (DPPBz

and DEPbZ) are powerful chelates and appear to generate the most-robust cationic cobalt(II) catalysts.

Three extended high-TO number hydroformylation runs were used to demonstrate the stability of the cationic cobalt(II) catalyst in a batch autoclave environment using very low catalyst loadings (table S10). The longest and highest TO run used 3 μM (0.24 ppm Co) [Co(acac)(DPPBz)](BF₄) and 6 M 1-hexene (45.45 g, 68 ml, 2 million equivalents) in 18 ml of dimethoxytetraglyme solvent. The reaction was run at 160°C under 50 bar of 1:1 H₂:CO for 14 days (336 hours). During this time, 1.2 million TOs to aldehyde product were performed with an average TOF of 59.5 min⁻¹. The product distribution at the end was 2% 1-hexene, 1.2%

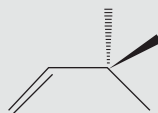
alkane, 40.8% isohexenes, 33.4% aldehyde (of which >50% was 2-methylhexanal), 1.1% alcohol, and 21.5% condensed aldehydes (mostly dimers, with some trimers). The catalyst was still operating after 336 hours, and the rate of hydroformylation at this point (55 TOs/min, GC-MS analysis) indicated excellent catalyst stability. With the exception of passing the 1-hexene through a short alumina column to remove peroxide impurities, no special purifications of the solvent, catalyst, or reaction gases were undertaken.

Evidence for a 19e⁻ intermediate

In situ Fourier-transform infrared (FTIR) studies using a Mettler Toledo ReactIR system with a high-pressure cell and a SiComp

Table 3. Hydroformylation of 3,3-dimethylbutene by cobalt and rhodium catalysts. All reactions were run with 1.0 M 3,3-dimethylbutene, 1.0 mM catalyst, 0.1 M heptane as internal standard, and 1:1 H₂:CO. Results are based on three runs with standard deviations given in parentheses; cobalt catalysts were run for 2 hours, and the rhodium catalysts were run for 20 min. The *k*_{obs} values were determined by gas consumption analysis under constant

pressure conditions. Cobalt precatalysts were introduced as the BF₄ salts in dimethoxytetraglyme solvent and activated at 160°C for 5 min, then cooled to operating temperature before the alkene was injected. Rh(acac)(CO)₂ was used as the catalyst precursor and run in toluene with the following excess phosphine:Rh ratios: 3:1 for the chelating biphenphos ligand and 400:1 for PPh₃:Rh. No excess phosphine was used for the cobalt runs.



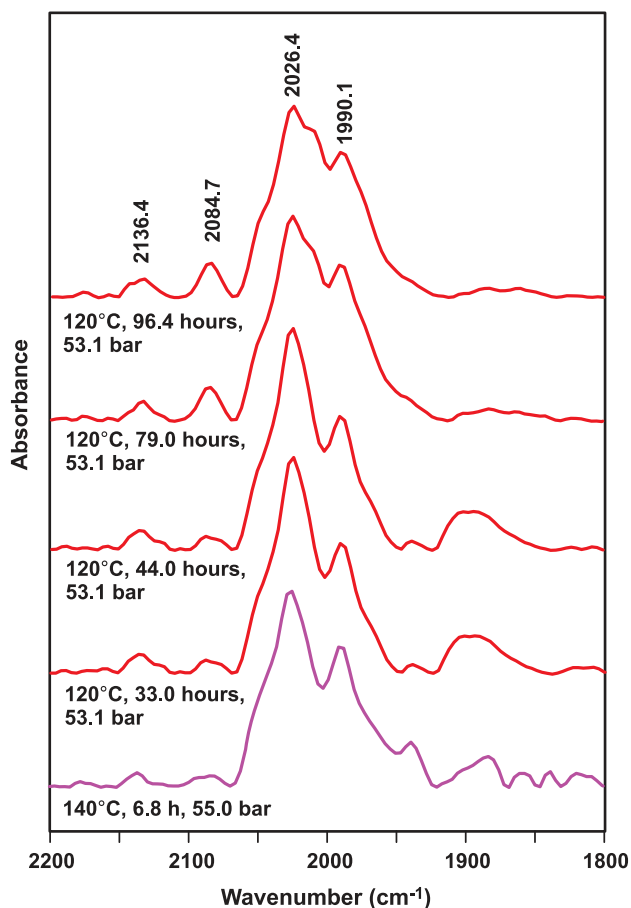
Catalyst	Temperature (°C)	Pressure (bar)	Time (min)	Aldehyde (%)	Aldehyde L:B	Alkane (%)	<i>k</i> _{obs} × 10 ⁻⁴ (M s ⁻¹)
[Co:DPPBz] ⁺	140	30	120	60.0 (3.8)	58	0.8 (0.02)	1.4 (2)
[Co:dpppe] ⁺	140	30	120	64.1 (3.5)	57	1.0 (0.1)	1.5 (1)
[Co:depe] ⁺	140	30	120	77.1 (1.0)	54	1.2 (0.05)	2.1 (1)
[Co:DEPBz] ⁺	140	30	120	84.8 (1.7)	51	1.2 (0.1)	2.6 (1)
Rh:biphenphos	120	15	20	96.4 (0.2)	All linear	3.3 (0.06)	25 (1)
Rh:PPh ₃	120	10.3	20	91.1 (2.1)	34	0.3 (0.04)	21 (2)

Table 4. Hydroformylation results for internal branched alkenes. All reactions were run for 6 hours with 1.0 M alkene, 1.0 mM catalyst, 0.1 M heptane as internal standard, and 1:1 H₂:CO. Results are an average of two runs. Co₂(CO)₈ or Co(hexanoate)₂ was used to generate HCo(CO)₄, and the cobalt reactions were run in dimethoxytetraglyme solvent. Rh(acac)(CO)₂ was used as the catalyst precursor and run in toluene with the following excess phosphine:Rh ratios: 3:1 for the chelating biphenphos ligand and 400:1 for PPh₃:Rh. No alcohol production was observed.

Alkene	Catalyst	Temperature (°C)	Pressure (bar)	Aldehyde (%)	Aldehyde L:B	Alkane (%)	Isomer (%)
	HCo(CO) ₄	140	90	36.5	All linear	–	4.8
	[Co:depe] ⁺	140	30	24.9	All linear	–	10.0
	Rh:biphenphos	120	15	0	–	–	–
	Rh:PPh ₃	120	10.3	0	–	–	–
	HCo(CO) ₄	140	90	28.6	All linear	2.2	14.2
	[Co:depe] ⁺	140	30	26.9	All linear	3.7	33.5
	Rh:biphenphos	120	15	0.8	All linear	–	2.8
	Rh:PPh ₃	120	10.3	0	–	–	–
	HCo(CO) ₄	140	90	77.7	6.2	–	10.4
	[Co:depe] ⁺	140	30	54.7	4.4	–	32.1
	Rh:biphenphos*	120	15	81.7*	28	1.9	14.8
	Rh:PPh ₃	120	10.3	62.0	0.4	–	8.4

*The Rh:biphenphos catalyst decomposed and stopped hydroformylating after 3 hours, as indicated by the absence of additional H₂:CO gas uptake.

Fig. 2. In situ FTIR studies of [Co(acac)(DPPBz)](BF₄). A 101-hour study of the cationic cobalt catalyst (10 mM) in dimethoxytetraglyme. The proposed catalyst complexes, [HCo(CO)_x(DPPBz)]⁺ (*x* = 1 to 3), have carbonyl bands at 2085, 2046 (shoulder), 2026, 2011 (shoulder), 1990, and 1974 cm⁻¹ (shoulder). The monometallic cationic cobalt-bisphosphine catalyst shows only minor changes in the carbonyl region upon stirring at 120°C and 53 bar for 65 hours. The band at 2136 cm⁻¹ is free CO dissolved in the solvent.



probe provided insight into the nature of the active catalyst and its high stability. Figure 2 shows representative FTIR spectra of the metal-carbonyl region between 120° and 140°C over the course of a 101-hour study for a 10 mM sample of [Co(acac)(DPPBz)](BF₄) in dimethoxytetraglyme solvent reacting with 1:1 H₂:CO. The catalyst precursor underwent hydrogenolysis at 120°C (more slowly at lower temperatures of 80° to 100°C) to lose acacH and generate the proposed mixture of cationic Co(II) hydrides: [HCo(CO)_x(DPPBz)]⁺, where *x* = 1 (15e⁻), 2 (17e⁻), and 3 (19e⁻). The formally 19e⁻ tricarbonyl complex is assigned to the highest-frequency coordinated carbonyl band observed at 2085 cm⁻¹, along with two other carbonyl bands in the 2046- to 2000-cm⁻¹ region [fig. S16 and density functional theory (DFT) assignments in table S12]. This species is most clearly observed in the IR at lower temperatures with enough dissolved CO present. All three monomeric catalyst species are in equilibrium across the temperature range studied, with terminal CO bands in the 2085- to 1980-cm⁻¹ range.

A similar cationic 17e⁻ Co(II) complex, [HCo(CO)₂(dippf)]⁺ [dippf, 1,1'-bis(diisopropylphosphino)ferrocene], has been prepared using electrochemical oxidation from the neutral

Co(I) species. Carbonyl bands are observed at 2051 and 2024 cm⁻¹ (24). The dippf ligand has a much larger chelate bite angle relative to DPPBz, so the structures of [HCo(CO)₂(dippf)]⁺ and [HCo(CO)₂(DPPBz)]⁺, neither of which have been determined, are expected to be different. One of our carbonyls is proposed to be trans to a phosphine ligand, which should result in a lower CO stretching frequency relative to that seen for [HCo(CO)₂(dippf)]⁺, which should not have any carbonyls trans to phosphine ligands. The higher frequency positions of the terminal bands are consistent between both cationic Co(II) complexes. [HCo(CO)₂(dippf)]⁺ disproportionates under the spectroelectrochemical conditions to eliminate H₂ and form the Co(I) complex [Co(CO)₂(dippf)]⁺.

High-pressure ¹H, ³¹P, and ⁵⁹Co nuclear magnetic resonance (NMR) studies (25, 26) of our catalyst (23° to 120°C, 27 bar, 1:1 H₂:CO) did not show any hydride, ³¹P, or ⁵⁹Co NMR resonances, which is consistent with the catalyst species being paramagnetic Co(II). No diamagnetic cobalt species were observed in the high-pressure NMR studies of the catalyst, which considerably reduces the likelihood that traditional Co(I) hydroformylation catalysts are involved. The high activity and medium-to-low pressure stability of this cationic catalyst system clearly argue against

HCo(CO)₄ or HCo(CO)₃(PR₃) catalyst formation or participation. Electron paramagnetic resonance (EPR) studies (fig. S9) demonstrate that the [Co(acac)(DPPBz)](BF₄) catalyst precursor is low-spin Co(II) with clear hyperfine coupling to one cobalt and two equivalent phosphorus centers, indicating a square planar geometry. This structure has been confirmed by x-ray crystallography (fig. S10) with a coordinated THF.

The in situ FTIR study summarized in Fig. 2 demonstrates that there are only minor changes in the carbonyl region of the catalyst at 120°C and 53 bar between the 33- and 96-hour spectra. After cooling and depressurization of the IR cell, the catalyst solution was transferred to an autoclave and was fully active for the hydroformylation of 1-hexene (140°C, 50 bar), giving the same catalytic results as a fresh catalyst precursor sample. This observation demonstrates very good catalyst stability under reaction conditions with no alkene substrate present. A simple industrial stability test for rhodium-phosphine hydroformylation catalysts involves stirring in an autoclave under 1:1 H₂:CO at the reaction temperature in the absence of alkene. All rhodium-phosphine catalysts with P-OR, P-phenyl, or P-benzyl linkages deactivate under these conditions via Rh-induced phosphine fragmentation reactions within 24 hours (usually less). The lower activity of our cobalt catalyst relative to rhodium appears to protect it from metal-induced phosphine ligand and catalyst degradation reactions. This, combined with a strong chelate effect that minimizes phosphine dissociation, produces a robust catalyst that does not require excess phosphine ligand for stability.

A proposed mechanism for this class of cationic Co(II) bisphosphine catalysts is shown in Fig. 3. The fundamental reaction steps are essentially the same as those for known hydroformylation catalysts: alkene coordination, migratory insertion of hydride to form the alkyl, and migratory insertion of CO with the alkyl to form an acyl-like species. Owing to the cationic charge and Co(II) oxidation state, the hydrogen reaction with the cobalt-acyl is proposed to be a heterolytic cleavage to eliminate aldehyde product and regenerate the cationic cobalt-hydride catalyst, as an oxidative addition of H₂ to form a cationic Co(IV) dihydride complex is unlikely.

Alkene coordination to the cobalt center is proposed to occur almost exclusively via the equatorial coordination site that is trans to the bisphosphine ligand. The axial coordination sites are less accessible to sterically hindered alkenes, such as those shown in Table 4. DFT calculations of the association of tetramethylethylene to the free coordination site favor equatorial over axial sites by ~4 kcal/mol (table S16). The most sterically accessible coordination site on the cobalt center is the equatorial

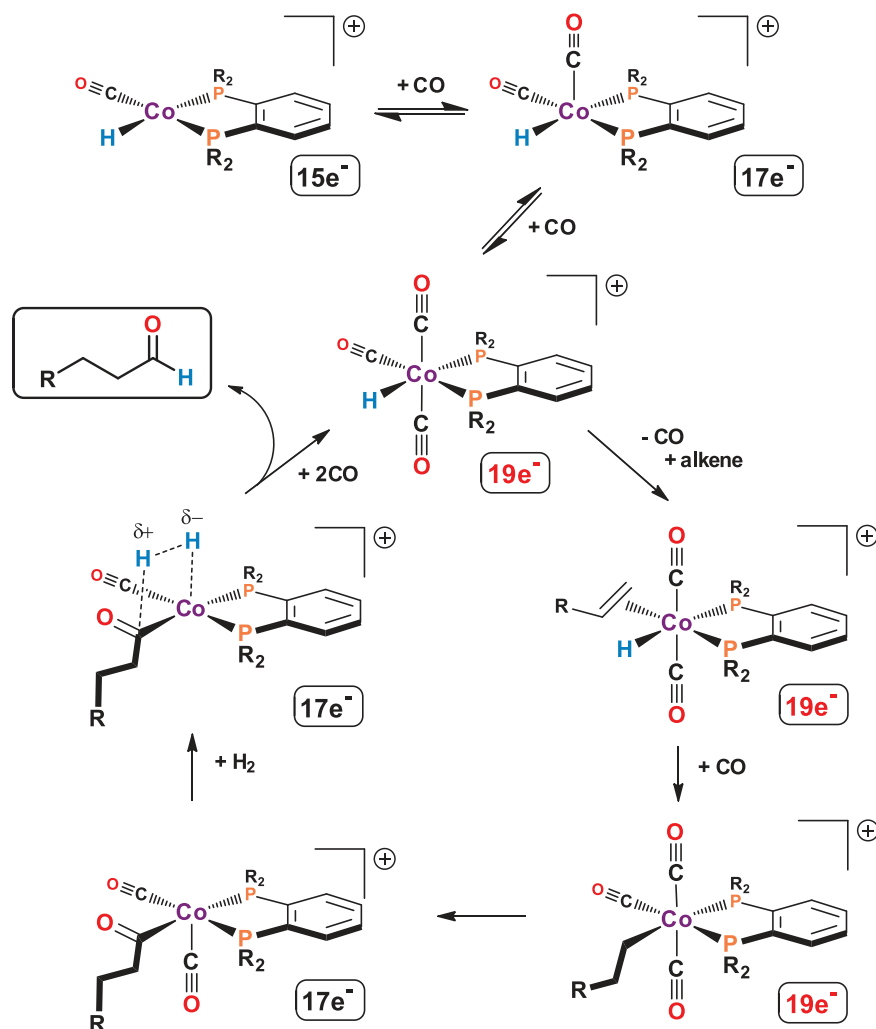


Fig. 3. Proposed hydroformylation mechanism involving $19e^-$ catalyst species. Most of the proposed reaction steps are entirely consistent with what is known for cobalt and rhodium hydroformylation catalysts. A distinctive key feature is the capacity to form $19e^-$ complexes via CO coordination, which helps weaken and dissociate the equatorial CO ligand, the strongest bound CO in the proposed alkene coordination site. The equatorial coordination site is the most likely binding site for sterically hindered alkenes. Although single reaction arrows are shown for clarity, each step is in equilibrium. δ^+ , partial positive charge; δ^- , partial negative charge.

carbonyl, but this is also the strongest CO binding site.

The coordination of a third CO ligand to form a 6-coordinate $19e^-$ complex helps weaken all the metal-ligand bonds, but especially the equatorial CO ligand that must dissociate to make room for an incoming alkene ligand. There is a much lower energy cost to form a $19e^-$ versus a $20e^-$ complex. Shi and colleagues demonstrated that the carbonyl substitution chemistry for $17e^-$ $V(CO)_6$ radical proceeds 10^{10} times faster than for $18e^-$ $Cr(CO)_6$ (27). The phosphine substitution reaction with the $17e^-$ $V(CO)_6$ radical was shown to be associative and extremely facile, proceeding through a $19e^-$ transition state. The $18e^-$ $[V(CO)_6]^-$ anion, in marked contrast, is inert toward phosphine substitution reactions. DFT calculations show that the $19e^-$

$[HCo(CO)_3(DPPBz)]^+$ complex is ~ 9 kcal/mol higher in free energy than the $17e^-$ complex at 115°C , indicating that its formation is energetically accessible (table S15).

The other important rate-enhancing effect is the cationic charge localized on the cobalt center, which compensates for the two donating phosphine ligands. Our work on the dicationic dirhodium tetraphosphine hydroformylation catalyst system has clearly shown the importance of having a localized cationic charge on the metal center to compensate for the electron-donating property of the two phosphine ligands (28). As seen for the neutral $Co(I)$ $HCo(CO)_3(PR_3)$ catalyst system, the electron-donating phosphine ligand enhances electron density at Co, which contributes to CO π -backbonding. This, in turn, increases the Co–CO bond strength, which stabilizes the catalyst with

respect to decomposition to cobalt metal but also substantially slows catalysis.

The $17e^-$ dicarbonyl complex, $[HCo(CO)_2(\text{bisphosphine})]^+$, may also coordinate alkene to the equatorial coordination site after CO dissociation to initiate hydroformylation. But the observed ligand effects on hydroformylation and observation of proposed $19e^-$ carbonyl complexes in the FTIR indicate that $19e^-$ intermediates likely play an important role in catalysis. This cationic $Co(II)$ -bisphosphine catalyst, for example, shows increased activity with more electron-donating phosphines at medium CO partial pressures (Table 3 and table S4). This observation further supports the proposed $19e^-$ intermediate that helps stabilize the equatorial Co–CO bond, allowing alkene coordination to initiate hydroformylation.

The high-energy carbonyl band around 2085 cm^{-1} is assigned to the $19e^-$ $[HCo(CO)_3(\text{bisphosphine})]^+$ complex. This band increases in intensity for the more electron-donating phosphine ligands studied (fig. S15). The more electron-rich bisphosphine ligands favor the $19e^-$ tricarbonyl complex at lower CO partial pressures, which in turn helps stabilize the equatorial carbonyl ligand under those conditions. As the CO partial pressure increases, the free CO in solution starts to compete with the alkene for coordination to the more electron-rich metal center, leading to the CO inhibition effect appearing sooner relative to the more electron-deficient bisphosphine ligands. Temperature also plays an important role in stabilizing the Co–CO ligands.

Monodentate phosphines (PBu_3 , PPh_3) do not generate effective hydroformylation catalysts under these medium-pressure conditions (table S8). Sterically bulky chelating bisphosphines such as $(iPr)_2PCH_2CH_2P(iPr)_2$ generate cationic $Co(II)$ hydroformylation catalysts that are considerably less active than the bisphosphine ligands reported here (table S9). One explanation is that the more hindered phosphine ligands inhibit addition of two axial CO ligands to form the key $19e^-$ $[HCo(CO)_3(P_2)]^+$ catalyst species that favors equatorial CO dissociation. The increased steric bulk of the bisphosphine isopropyl or cyclohexyl groups has little effect on the aldehyde L:B ratio (table S9 and figs. S17 and S18), which supports the proposed equatorial coordination of the alkene into the least sterically hindered metal coordination site. The bisphosphine R groups are pointed away from the equatorial plane and most affect axial ligand coordination. This is another piece of evidence supporting the $19e^-$ catalyst species as an important player in the catalytic mechanism.

Outlook

Relatively little research into new cobalt-based hydroformylation catalysts has occurred since the introduction of the phosphine-modified

catalyst system in the late 1960s. The combination of relatively high pressures and temperatures needed, along with the assumption that industry had explored most alternative cobalt hydroformylation catalysts, strongly inhibited research in this area. The discovery of this highly active cationic Co(II) hydroformylation catalyst system was therefore quite surprising. That this catalyst system appears to have exceptional stability with respect to cobalt-induced phosphine degradation reactions or decomposition to cobalt metal opens doors for medium-pressure hydroformylation technology in both academic and industrial settings.

REFERENCES AND NOTES

1. A. Börner, R. Franke, *Hydroformylation: Fundamentals, Processes, and Applications in Organic Synthesis* (Wiley-VCH, 2016).
2. I. Wender, P. Pino, *Organic Syntheses via Metal Carbonyls*, vol. 2 (Wiley, 1977), pp. 47–197.
3. F. Hebrard, P. Kalck, *Chem. Rev.* **109**, 4272–4282 (2009).
4. R. F. Heck, D. S. Breslow, *J. Am. Chem. Soc.* **82**, 4438–4439 (1960).
5. R. F. Heck, D. S. Breslow, *J. Am. Chem. Soc.* **83**, 4023–4027 (1961).
6. B. Cornils, in *New Syntheses with Carbon Monoxide*, J. Falbe, Ed. (Springer-Verlag, 1980).
7. L. H. Slaugh, R. D. Mullineaux, *J. Organomet. Chem.* **13**, 469–477 (1968).
8. L. H. Slaugh, R. D. Mullineaux, Hydroformylation of olefins, U.S. Patent 3,448,157 (1969).
9. D. Evans, J. A. Osborn, G. Wilkinson, *J. Chem. Soc. A* **1968**, 3133–3142 (1968).
10. R. L. Pruett, J. A. Smith, *J. Org. Chem.* **34**, 327–330 (1969).
11. C. Li, L. Guo, M. Garland, *Organometallics* **23**, 2201–2204 (2004).
12. P. W. N. M. van Leeuwen, C. P. Casey, G. T. Whiteker, in *Rhodium Catalyzed Hydroformylation*, P. W. N. M. van Leeuwen, C. Claver, Eds. (Kluwer, 2000).
13. M. E. Broussard *et al.*, *Science* **260**, 1784–1788 (1993).
14. D. A. Aubry, N. N. Bridges, K. Ezell, G. G. Stanley, *J. Am. Chem. Soc.* **125**, 11180–11181 (2003).
15. W. J. Schreiter *et al.*, *Inorg. Chem.* **53**, 10036–10038 (2014).
16. S. Pandey *et al.*, *J. Am. Chem. Soc.* **140**, 4430–4439 (2018).
17. E. Billig, A. G. Abatjoglou, D. R. Bryant, Transition metal complex catalyzed processes, U.S. Patent 4,668,651 (1988).
18. B. Moasser, W. L. Gladfelder, D. C. Roe, *Organometallics* **14**, 3832–3838 (1995).
19. G. W. Parshall, W. H. Knoth, R. A. Schunn, *J. Am. Chem. Soc.* **91**, 4990–4995 (1969).
20. Rhodium and cobalt metal prices: www.dailymetalprice.com.
21. P. W. N. M. van Leeuwen, C. F. Roobeek, *J. Organomet. Chem.* **258**, 343–350 (1983).
22. A. G. Abatjoglou, E. Billig, D. R. Bryant, *Organometallics* **3**, 923–926 (1984).
23. A. G. Abatjoglou, D. R. Bryant, *Organometallics* **3**, 932–934 (1984).
24. M. J. Krafft *et al.*, *Angew. Chem. Int. Ed.* **52**, 6781–6784 (2013).
25. R. J. Klingler, J. W. Rathke, *J. Am. Chem. Soc.* **116**, 4772–4785 (1994).
26. M. J. Chen, R. J. Klingler, J. W. Rathke, K. W. Kramarz, *Organometallics* **23**, 2701–2707 (2004).
27. Q.-Z. Shi, T. G. Richmond, W. C. Troglor, F. Basolo, *J. Am. Chem. Soc.* **106**, 71–76 (1984).
28. R. C. Matthews *et al.*, *Angew. Chem. Int. Ed.* **35**, 2253–2256 (1996).

ACKNOWLEDGMENTS

We thank D. P. Young (LSU Physics) for collecting magnetic susceptibility data on [Co(acac)(DEPBz)](BF₄) and [Co(acac)(DPPBz)](BF₄). **Funding:** The authors gratefully acknowledge the following financial support, which led to this research: prior support from U.S. National Science Foundation grant CHE-01-11117, Dow Chemical, Louisiana Board of Regents LEQSF(2014-17)-RD-B-02, and LSU LIFT²; and current support from ExxonMobil

Chemical Company. **Author contributions:** D.M.H. designed and prepared all the original catalyst precursors; performed catalytic testing and high-pressure in situ NMR studies; and assisted with the high-pressure FTIR studies and low- and high-pressure EPR sample preparation. R.A.J. independently tested the catalysts, collected data with different substrates, and assisted with the high-pressure FTIR studies. A.E.C. independently prepared and tested the cationic cobalt catalyst and performed x-ray crystallographic studies. J.M.Y. performed DFT calculations on low- and high-spin variants of the cationic cobalt(II) catalysts. D.J.V. collected and interpreted all the EPR data on the [Co(acac)(DPPBz)](BF₄) catalyst precursor and activated catalyst under low- and high-pressure H₂/CO conditions. G.G.S. designed the cationic catalyst concept for hydroformylation; performed the high-pressure FTIR experiments and separate DFT studies on the catalyst species; and contributed to the interpretation of the results and primary drafting of the paper. **Competing interests:** D.M.H. and G.G.S. are inventors on PCT patent application PCT/US19/36194 submitted by Louisiana State University, which covers this and related catalyst systems. A.E.C. and J.M.Y. are employees of ExxonMobil Chemical Company. **Data and materials availability:** Crystallographic data for [Co(acac)(THF)(DPPBz)](BF₄) are freely available from the Cambridge Crystallographic Data Centre under CCDC-1957261. Full synthetic and catalytic details, including preparative procedures and spectroscopic data for catalyst precursors, along with additional catalytic results, can be found in the supplementary materials. Optimized DFT geometries and energetics are provided as a separate zipped tarball (DFT_structures.tar.gz; see supplementary materials).

SUPPLEMENTARY MATERIALS

science.sciencemag.org/content/367/6477/542/suppl/DC1
Materials and Methods
Figs. S1 to S19
Tables S1 to S16
References (29–50)
DFT Geometries

5 August 2019; accepted 23 December 2019
10.1126/science.aaw7742

Highly active cationic cobalt(II) hydroformylation catalysts

Drew M. Hood, Ryan A. Johnson, Alex E. Carpenter, Jarod M. Younker, David J. Vinyard and George G. Stanley

Science **367** (6477), 542-548.
DOI: 10.1126/science.aaw7742

Charging up cobalt for hydroformylation

Hydroformylation reactions are applied at massive scale in the chemical industry to transform olefins into aldehydes. The original catalysts were neutral cobalt complexes. Hood *et al.* now report that positively charged cobalt complexes, stabilized by chelating phosphine ligands, show higher activities at lower pressures than their neutral counterparts, approaching the activities of precious rhodium catalysts. These charged catalysts are particularly adept at accelerating the reactions of internal olefins while avoiding decomposition. Spectroscopic studies implicate the involvement of 19-electron intermediates in the catalytic cycle.

Science, this issue p. 542

ARTICLE TOOLS

<http://science.sciencemag.org/content/367/6477/542>

SUPPLEMENTARY MATERIALS

<http://science.sciencemag.org/content/suppl/2020/01/29/367.6477.542.DC1>

REFERENCES

This article cites 42 articles, 1 of which you can access for free
<http://science.sciencemag.org/content/367/6477/542#BIBL>

PERMISSIONS

<http://www.sciencemag.org/help/reprints-and-permissions>

Use of this article is subject to the [Terms of Service](#)

Science (print ISSN 0036-8075; online ISSN 1095-9203) is published by the American Association for the Advancement of Science, 1200 New York Avenue NW, Washington, DC 20005. The title *Science* is a registered trademark of AAAS.

Copyright © 2020 The Authors, some rights reserved; exclusive licensee American Association for the Advancement of Science. No claim to original U.S. Government Works